Hindawi
Complexity
Volume 2022, Article ID 6279373, 14 pages
https://doi.org/10.1155/2022/6279373

Research Article

A Novel Highly Nonlinear Quadratic System: Impulsive Stabilization, Complexity Analysis, and Circuit Designing

Arthanari Ramesh,[1] **Alireza Bahramian**,[2] **Hayder Natiq**,[3] **Karthikeyan Rajagopal**,[4] **Sajad Jafari**,[2,5] **and Iqtadar Hussain**[6,7]

[1]*Centre for Materials Research, Chennai Institute of Technology, Chennai, India*
[2]*Department of Biomedical Engineering, Amirkabir University of Technology (Tehran Polytechnic), Tehran, Iran*
[3]*Information Technology Collage, Imam Ja'afar Al-Sadiq University, 10001 Baghdad, Iraq*
[4]*Centre for Nonlinear Systems, Chennai Institute of Technology, Chennai, India*
[5]*Health Technology Research Institute, Amirkabir University of Technology (Tehran Polytechnic), Tehran, Iran*
[6]*Mathematics Program, Department of Mathematics, Statistics and Physics, College of Arts and Sciences, Qatar University, 2713 Doha, Qatar*
[7]*Statistical Consulting Unit, College of Arts and Science, Qatar University, Doha, Qatar*

Correspondence should be addressed to Karthikeyan Rajagopal; rkarthiekeyan@gmail.com

Received 20 June 2021; Revised 16 February 2022; Accepted 17 February 2022; Published 30 March 2022

Academic Editor: M. De Aguiar

This work introduces a three-dimensional, highly nonlinear quadratic oscillator with no linear terms in its equations. Most of the quadratic ordinary differential equations (ODEs) such as Chen, Rossler, and Lorenz have at least one linear term in their equations. Very few quadratic systems have been introduced and all of their terms are nonlinear. Considering this point, a new quadratic system with no linear term is introduced. This oscillator is analyzed by mathematical tools such as bifurcation and Lyapunov exponent diagrams. It is revealed that this system can generate different behaviors such as limit cycle, torus, and chaos for its different parameters' sets. Besides, the basins of attractions for this system are investigated. As a result, it is revealed that this system's attractor is self-excited. In addition, the analog circuit of this oscillator is designed and analyzed to assess the feasibility of the system's chaotic solution. The PSpice simulations confirm the theoretical analysis. The oscillator's time series complexity is also investigated using sample entropy. It is revealed that this system can generate dynamics with different sample entropies by changing parameters. Finally, impulsive control is applied to the system to represent a possible solution for stabilizing the system.

1. Introduction

Chaos is a complex behavior that has been investigated in nature and mathematics [1]. It refers to the systems' sensitivity to their initial conditions and parameters [2]. Nonlinear systems such as ordinary differential equations (ODEs) can generate chaotic behavior [3]. Therefore, they can have applications in modeling natural systems with chaotic behaviors such as neurons [4]. Besides, using coupling methods, these systems can investigate collective behaviors of neuronal networks [5]. It is good to mention that sometimes these dynamical systems are used in their nonchaotic mode to model some behaviors of natural systems like central pattern generators (neurons that make rhythms for locomotions) [6]. ODEs chaotic systems have been categorized based on their equilibrium points types and locations [7]. In this way, chaotic systems' attractors can be divided into two groups: ones that have at least one equilibrium point in their basin of attraction (self-excited attractors) [8] and ones that have no equilibrium point in their basin of attraction (hidden attractor(s)) [9]. Besides, the systems' equilibrium points are interesting nonlinear dynamics properties for researchers. For example, systems have been introduced and investigated with a line of

equilibria [9] or just one stable equilibrium [10]. Besides, two main groups of systems can be defined based on the equations' time dependency: autonomous systems in which no term as a function of time exists in their equations [11] and nonautonomous systems in which a term dependent to the time can be found in their equations (forced systems) [12]. Besides, forcing systems can lead nonchaotic oscillators to systems that have the capability of generating chaos. For instance, using this technique, two-dimensional systems that cannot generate chaotic time series can demonstrate chaotic attractors [13]. These nonautonomous systems are also capable of generating hidden attractors [14]. Another method to make a system chaotic is considering delays in the equations of the system. For instance, a system with just one equation can make chaos if it has a time delay in its equation [15]. On the other hand, systems with four dimensions or more can generate hyperchaotic behaviors. For instance, a four-dimensional jerk system implicated with memristors has shown the potential of demonstrating hyperchaos [16]. Besides these features, multistability refers to the existence of several attractors (at least two ones) for different initial values for a system without parameters' changing [17]. In addition to the mentioned properties, some other features are defined for chaotic systems based on the topology and shapes of attractors [18]. Some strange attractors with different symmetries' types were reported [19]. Besides, the systems with several wings' attractors (multiscrolls) have grabbed researchers' interest [20]. For instance, it is investigated how the strange multiscrolls attractor for a system can emerge and how its shape can be preserved [21]. In addition, the systems that their attractors look like known objects were also reported. For instance, chaotic systems have been introduced to look like a Persian carpet [22] or a peanut [23].

Among different ODE systems, quadratic ones are mainly focused on by some researchers interested in finding elegant systems [2]. One reason is that these systems can have simpler equations [24]. Lorenz equations, the first introduced chaotic system, are one of these classes and have just quadratic terms. Some quadratic systems were introduced whose equations' terms are lower than that of the Lorenz equations [24]. Various dynamics of a quadratic system were studied in [25]. Most of the quadratic systems have at least one linear term in one of their equations [26]. Few systems have been introduced with no linear term in their equations [27]. Xu and Wang introduced such a system built by just nonlinear quadratic terms for the first time [28]. As another example of the pure nonlinear systems category, a multistable system can be mentioned with heterogeneous attractors [29]. Here, an oscillator with absolute nonlinear terms is introduced to generate various types of nonlinear dynamics' behaviors such as torus and chaos.

The chaotic feasibility of nonlinear ODEs systems always has been a question. Designing analog circuits for chaotic systems has been a hot topic recently. Electrical circuits simulated with PSpice or implemented physically are tools to assess ODE systems' chaotic behaviors. For example, an electrical circuit was introduced to regenerate the chaotic signals with a multiscroll dynamic [30]. In another instance, analog electrical circuits of a system with multistability were impacted [23]. Using memristors to model chaotic dynamics is one of the hot topics; for instance, a five-dimensional system with three linear dimensions was implicated using two memristors [1]. Besides, chaotic systems' implication using digital circuits like field-programmable gate array (FPGA) has been carried out to assess the possibility of implicating chaotic systems. For instance, a jerk system feasibility with strange coexisting attractors was assessed with FPGA [31]. In another example, the chaotic time series of a system with coexisting attractors and strange fixed points' curves was regenerated using FPGA [23]. One of the applications of these circuits is random number generation [32]. Other applications can be secure communications [33] and image encryption [34]. In this work, the system's analog circuit is designed with PSpice, and the results of simulations are reported.

The complexity of chaotic systems' signals has recently become an exciting subject for researchers [35]. For instance, the complexities of a system with hidden attractors (for time series of its different parameters' values) were calculated and discussed [36]. Sample entropy is a feature for comparing the complexity of time series repetitively [37]. In this method, the philosophy of calculating complexity is based on the possibility of predicting the future of the signals based on their previous samples [37]. This method has some advantages in comparison with other methods of measuring complexity. For instance, it is less dependent on the length of time series than approximated entropy [37]. Here, sample entropy is used for calculating the complexities of the oscillator's signals for different ranges of the introduced system's parameters.

Controlling chaotic oscillators has been an interesting topic [38]. Various methods have been proposed to control the chaotic dynamics [39, 40]. Impulsive control is a method of stabilizing nonlinear systems such as the ones with infinite [41, 42] or finite delays [43], delayed neural networks [44] (that also includes exponentially stabilization [45] and fixed time control [46]), stochastic delayed systems [47], or singularly perturbed models [48]. For instance, it was used for stabilizing systems whose states are not measurable [49]. In another example, an event-based version of this method was used for controlling Chua-coupled systems [50]. This method also has been used for synchronization among nonlinear systems [51], switched complex networks [52, 53], high-dimensional Kuramoto systems [54], and fuzzy neural networks [55]. Some advanced methods of impulsive control have been introduced, for instance, versions with adaptable frequencies [56]. In this paper, an impulsive-based method for controlling the introduced pure nonlinear system is implicated as a possible solution for stabilizing its equilibrium points.

In the next section, the system's equations whose terms are all nonlinear quadratic are presented (Section 2). Also, the oscillator's bifurcation and Lyapunov diagrams for different parameters' values are analyzed. Besides, the basin of attractions of the pure nonlinear oscillator is plotted and discussed. Section 3 explains the design of the introduced pure nonlinear oscillator's analog circuit and its

simulations with PSpice. The next part assesses the complexity of the oscillator's signals for various parameter values (Section 4). Applying the impulsive control method (Section 5) to the proposed system helps to enhance its applications. The simulations' results are concluded in the final part (Section 6).

2. The Highly Nonlinear System: Analytical and Numerical Analysis

The construction of chaotic dynamics is an unknown subject that attracted lots of attention [3, 57]. After revealing some counterexamples for the hypothesis of a relation between saddle equilibrium points and chaotic attractors [58, 59], many works have been focused on studying chaotic flows with unique properties [60, 61]. They have tried to understand the construction of chaotic attractors. Some examples are chaotic flows with different equilibrium points [62, 63] and special attractors [64]. So, a pure nonlinear chaotic flow is proposed here, and its various dynamics are investigated. The oscillator can be described by three-dimension equations that are coupled as follows:

$$\begin{aligned}\dot{x} &= 1.3z^2 - y^2 + a\dot{y}\\ &= y^2 - x^2\dot{z}\\ &= y^2 - x^2 + 0.1z^2 + b,\end{aligned} \tag{1}$$

where x, y, and z are the system's variables when a and b are considered parameters. The system is symmetric with the change of variables $(x, y, x, t) \longrightarrow (-x, -y, -z, -t)$. So any attractor of system (1) has a twin in reversed time and is symmetric to the origin of the main attractor. The system's equilibrium points are as follows:

$$\begin{aligned}0 &= 1.3z^2 - y^2 + a,\\ X &= \pm\sqrt{-13b + a},\\ 0 &= y^2 - x^2 \longrightarrow Y = \pm\sqrt{-13b + a},\\ 0 &= y^2 - x^2 + 0.1z^2 + b,\\ Z &= \pm\sqrt{-10b}.\end{aligned} \tag{2}$$

Considering these eight fixed points, the system's Jacobian and eigenvalues are as follows:

$$J = \begin{bmatrix} 0 & -2Y & 2.6Z \\ -2X & 2Y & 0 \\ -2X & 2Y & 0.2Z \end{bmatrix} \longrightarrow |\lambda I - J| = 0 \longrightarrow \begin{bmatrix} \lambda & 2Y & -2.6Z \\ 2X & \lambda - 2Y & 0 \\ 2X & -2Y & \lambda - 0.2Z \end{bmatrix} \longrightarrow \tag{3}$$
$$\lambda((\lambda - 2Y)(\lambda - 0.2Z) - 0) - 2Y(2X(\lambda - 0.2Z)) - 2.6Z(-4XY - (2X(\lambda - 2Y))) = 0.$$

The types of equilibria when $a = 0.5$ and $b = -2.3$ are shown in Table 1 (considering eigenvalues for each equilibrium).

The system's attractors for different parameters' values have been presented in Figure 1. Figures 1(a)–1(d) demonstrate periods 1, 2, 4 and chaotic behaviors of the oscillator.

The Lyapunov exponent and bifurcation diagrams for different parameters' set are calculated to investigate more about possible behaviors that the introduced system can present. Firstly the b parameter is fixed ($b = -2.3$), and Lyapunov and bifurcation diagrams for a range of a are plotted (Figure 2). Figure 2(a) demonstrates two Lyapunov exponents that have higher values than the rest. The third Lyapunov exponent's values are always negative and have a higher absolute value than the two others. For the two Lyapunov with higher values, the system's behavior is periodic when one is zero and the other is negative. For the situation that one of them is zero and another is positive, the system's behavior is chaotic. When both are zero, the system's behavior is the torus. Figure 2(a) demonstrates all of the mentioned situations; therefore, the system has the capability of having limit cycles, torus, and chaotic solutions. Figure 2(b) is the bifurcation diagram for the same range of a . Period windows can be seen in Figure 2(b). In the bifurcation diagram, a period-doubling route to chaos can be observed by decreasing parameter a.

In the next step, parameter a is fixed, and the oscillator's behaviors for various b are investigated. Figure 3 reveals the Lyapunov exponent and bifurcation diagrams when $a = 0.5$ and the b's value changes. For better visualization, the Lyapunov exponent with the largest absolute value (its value is always negative) is not plotted in Figure 3(a). The system's different behaviors from different limit cycles' periods to torus and chaos can be seen based on the previously explained situations of the two larger Lyapunov exponents (Figure 3(a)). An inverse route of the period-doubling route to chaos can be observed in the bifurcation diagram by increasing b (Figure 3(b)).

The basin of attractions when the oscillator's parameters are set $a = 0.5$ and $b = 2.3$ are plotted for a range of initial values (Figure 4). Two surfaces each containing four equilibrium points are plotted. Studying the basin of attraction of the oscillator shows that the oscillator has only one attractor. Figures 4(a) and 4(b) show the parts of plates that $Z = \sqrt{23}$ and $Z = -\sqrt{23}$, respectively. The equilibrium points $(X = +\sqrt{30.4}, Y = +\sqrt{30.4}, Z = +\sqrt{23})$ and $(X = -\sqrt{30.4}, Y = -\sqrt{30.4}, Z = -\sqrt{23})$ are located at the edge of the unstable region and the basin of attraction. The type of both of them is unstable (spiral). It can be seen that some equilibrium points exist in the system's attractor's basin of attraction. Therefore, the system's attractor is self-excited.

In the next section, an analog circuit of the system is implicated for the system when it is in its chaotic mode.

Table 1: The pure nonlinear system's equilibrium points and their related eigenvalues when $a = 0.5$ and $b = -2.3$ are set. The equilibria types are determined based on their eigenvalues.

Equilibrium points	Eigenvalues	Types
$X = +\sqrt{30.4}, Y = +\sqrt{30.4}, Z = +\sqrt{23}$	$\lambda_{1,2} \approx 7.0371 \pm 2.5182i,\ \lambda_3 \approx -2.0879$	Unstable (spiral)
$X = -\sqrt{30.4}, Y = +\sqrt{30.4}, Z = +\sqrt{23}$	$\lambda_{1,2} \approx -0.5447 \pm 2.9365i,\ \lambda_3 \approx 13.0757$	Unstable (spiral)
$X = +\sqrt{30.4}, Y = -\sqrt{30.4}, Z = +\sqrt{23}$	$\lambda_{1,2} \approx -5.2642 \pm 15.0219i,\ \lambda_3 \approx 0.4603$	Unstable (spiral)
$X = +\sqrt{30.4}, Y = +\sqrt{30.4}, Z = -\sqrt{23}$	$\lambda_1 \approx 22.3613, \lambda_2 \approx -11.8532, \lambda_3 \approx -0.44$	Unstable (saddle)
$X = -\sqrt{30.4}, Y = -\sqrt{30.4}, Z = +\sqrt{23}$	$\lambda_1 \approx -22.3613, \lambda_2 \approx 11.8532, \lambda_3 \approx 0.44$	Unstable (saddle)
$X = +\sqrt{30.4}, Y = -\sqrt{30.4}, Z = -\sqrt{23}$	$\lambda_{1,2} \approx 0.5447 \pm 2.9365i,\ \lambda_3 \approx -13.0757$	Unstable (spiral)
$X = -\sqrt{30.4}, Y = +\sqrt{30.4}, Z = -\sqrt{23}$	$\lambda_{1,2} \approx 5.2642 \pm 15.0219i,\ \lambda_3 \approx -0.4603$	Unstable (spiral)
$X = -\sqrt{30.4}, Y = -\sqrt{30.4}, Z = -\sqrt{23}$	$\lambda_{1,2} \approx -7.0371 \pm 2.5182i,\ \lambda_3 \approx 2.0879$	Unstable (spiral)

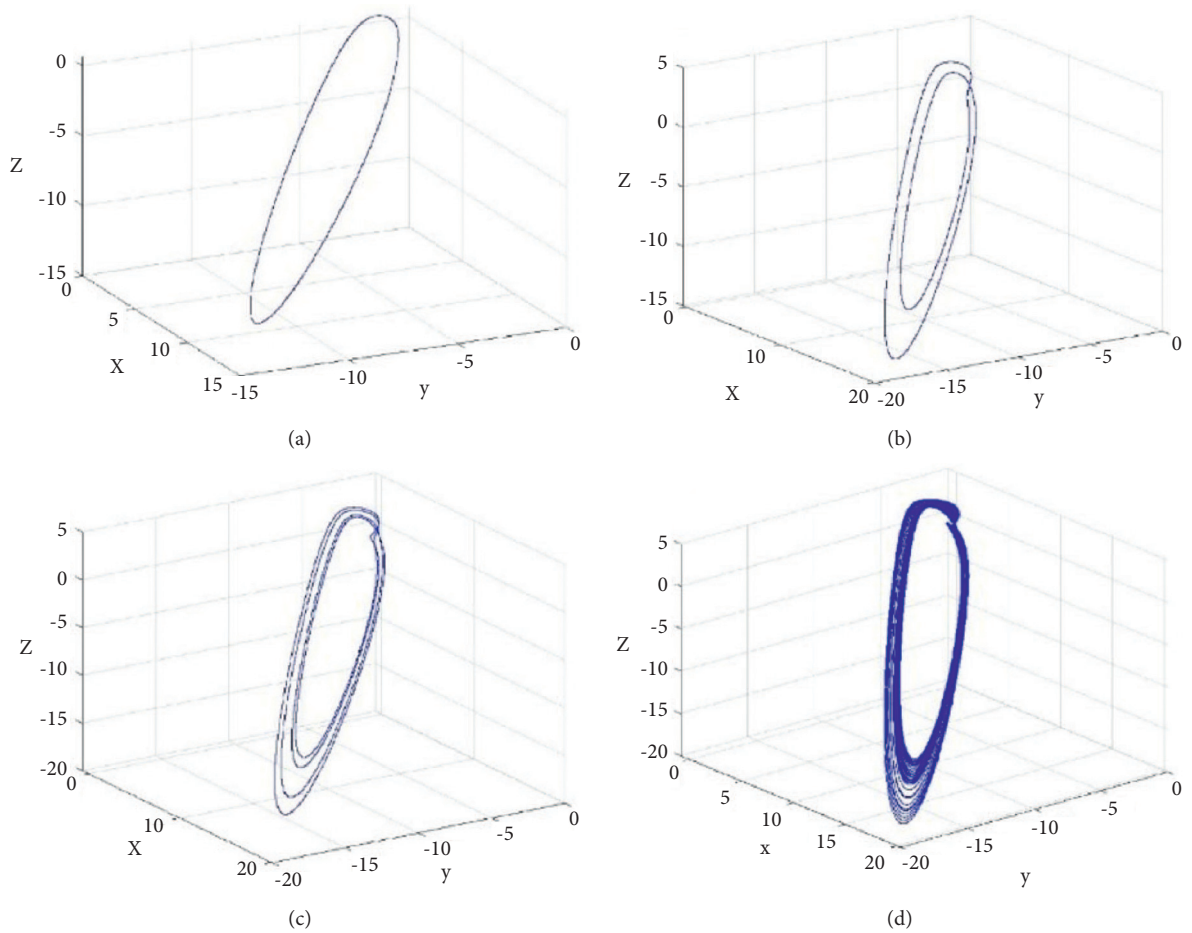

Figure 1: The systems' attractors for a's different values when $b = -2.3$. (a) For $a = 3$, period 1 can be seen in the system's attractor. (b) For $a = 2$, period 2 can be seen in the system's attractor. (c) For $a = 1.5$, period 3 can be seen in the system's attractor. (d) When $a = 1.1$, the oscillator's behavior is chaotic.

3. Analog System's Circuit, Design, and PSpice Implication

The pure nonlinear system's analog circuit in the chaotic mode is designed. Simple elements such as resistors and Op-Amps are used in its designed circuit. Its circuit's schematic is demonstrated in Figure 5. AD633/AD as an analog device is used for multiplying variables together. The values of capacitors and resistors are tuned to compensate for the mentioned coefficient. To avoid the analog devices' saturation,

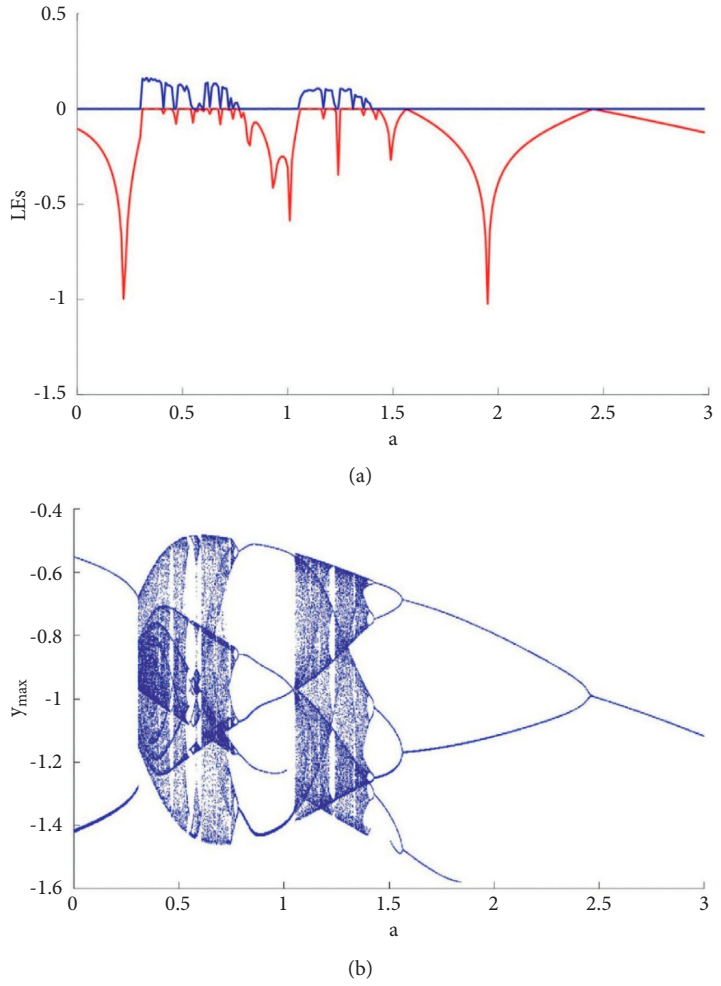

Figure 2: Lyapunov exponents and bifurcation diagrams for different a values. (a) The systems' two larger Lyapunov exponents are plotted. Periodic behaviors (one Lyapunov exponent negative and one zero), torus behaviors (when both Lyapunov exponents are zero), and chaotic behavior (one Lyapunov exponent is zero and another one is positive) can be seen in the diagram. (b) The bifurcation diagram of the system is plotted when the period-doubling route to chaos (from right to left) and period windows can be observed in the diagram.

$x = 10X$, $y = 10Y$, $z = 10Z$, and $t = 0.1T$ are considered. Therefore, the system's equations can be rewritten as follows:

$$\begin{aligned}
\frac{\mathrm{d}(10X)}{\mathrm{d}(0.1T)} &= 1.3(10z)^2 - (10Y)^2 + a \longrightarrow \frac{\mathrm{d}X}{\mathrm{d}T} = 1.3Z^2 - Y^2 + \frac{a}{100}, \\
\frac{\mathrm{d}(10Y)}{\mathrm{d}(0.1T)} &= (10Y)^2 - (10X)^2 \longrightarrow \frac{\mathrm{d}Y}{\mathrm{d}T} = Y^2 - X^2, \\
\frac{\mathrm{d}(10z)}{\mathrm{d}(0.1T)} &= (10Y)^2 - (10X)^2 + 0.1(10z)^2 + b \longrightarrow \frac{\mathrm{d}Z}{\mathrm{d}T} = Y^2 - X^2 + 0.1Z^2 + \frac{b}{100}.
\end{aligned} \tag{4}$$

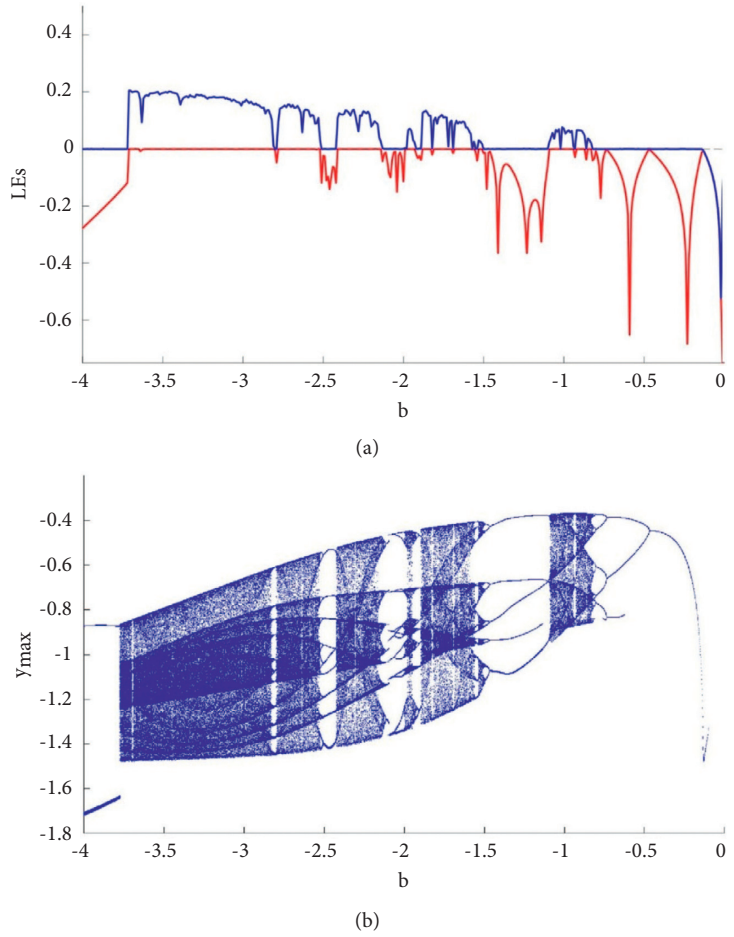

Figure 3: Lyapunov exponents and bifurcation diagrams when a value is fixed ($a = 0.5$). (a) For a range of b, the two largest Lyapunov exponents are potted. Based on these Lyapunov exponents' values, the system's behaviors (torus when both are zero, chaos when one is zero and another is positive, and periodic when one is negative and another is zero) for each specific value of b can be determined. (b) Bifurcation diagrams of the system for the b's same range. Period-doubling route to chaos (from right side to the left) and periodic windows can be seen in the diagram.

The new version of the system's equation (Eq. (4)) is designed by analog elements (Figure 5). The values of the analog elements are as follows: $R1 = 10K\Omega$, $R2 = 10K\Omega$, $R3 = 10K\Omega$, $R4 = 10K\Omega$, $R5 = 1K\Omega$, $R6 = 10K\Omega$ $R7 = 10K\Omega$, $R8 = 10K\Omega$, $R9 = 10K\Omega$, $R10 = 1K\Omega$, $R11 = 10K\Omega$, $R12 = 1K\Omega$ and $R13 = 1K\Omega$, $R14 = 1K\Omega$, $R15 = 13K\Omega$, $R16 = 1K\Omega$, $R17 = 1K\Omega$, $C1 = 10n$F, $C2 = 10n$F, $C3 = 10n$F. Finally, the implicated system's equation to simulate in PSpice can be written as follows:

$$\begin{aligned}
\frac{dX}{dT} &= \left(\frac{C1}{R1}\right)\left(\frac{R15}{R14}\right)\left(0.1Z^2\right) - \left(\frac{C1}{R2}\right)\left(\frac{R11}{R10}\right)\left(\frac{R13}{R12}\right)\left(0.1Y^2\right) + \left(\frac{C1}{R2}\right)V1, \\
\frac{dY}{dT} &= \left(\frac{C2}{R4}\right)\left(\frac{R11}{R10}\right)\left(0.1Y^2\right) - \left(\frac{C2}{R5}\right)\left(0.1X^2\right), \\
\frac{dZ}{dT} &= \left(\frac{C3}{R7}\right)\left(\frac{R11}{R10}\right)\left(0.1Y^2\right) - \left(\frac{C3}{R7}\right)\left(0.1X^2\right) + \left(\frac{R17}{R16}\right)\left(\frac{C3}{R9}\right)\left(0.1Z^2\right) + \left(\frac{C3}{R9}\right)V2.
\end{aligned} \tag{5}$$

The circuit simulation in PSpice when $a = 0.5$ and $b = -3.7$ is demonstrated in Figure 5. All elements that are used are analog. The outputs of the designed analog circuit compared to Matlab simulations are demonstrated in Figure 6.

4. The Pure Nonlinear System's Complexity Analysis

Defining the complexity of the time series based on their predictability results in the definition of sample entropy

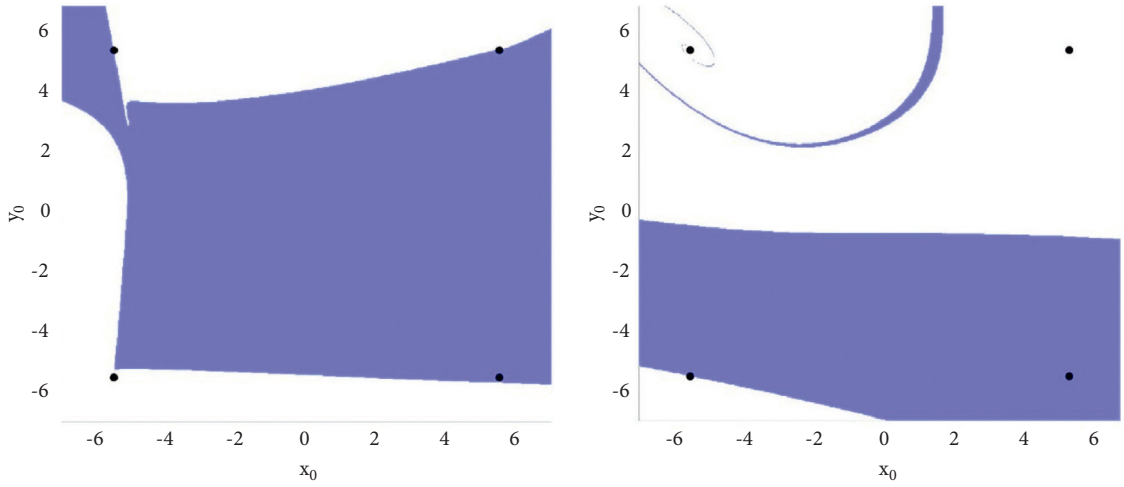

Figure 4: The system's basin of attractions ($a = 0.5$ and $b = 2.3$). According to our best search, the system has just one attractor. Different initial values of the systems are attracted to the attractor or have unbounded responses. White color is considered for plotting in both (a) and (b) parts for the initial values with unbounded responses. Regions that are attracted to the attractor are plotted with blue color. (a) and (b) are responsible for plates that $Z = \sqrt{23}$ and $Z = -\sqrt{23}$, respectively. Because some equilibrium points can be found in blue regions, the system can be categorized in the self-excited class.

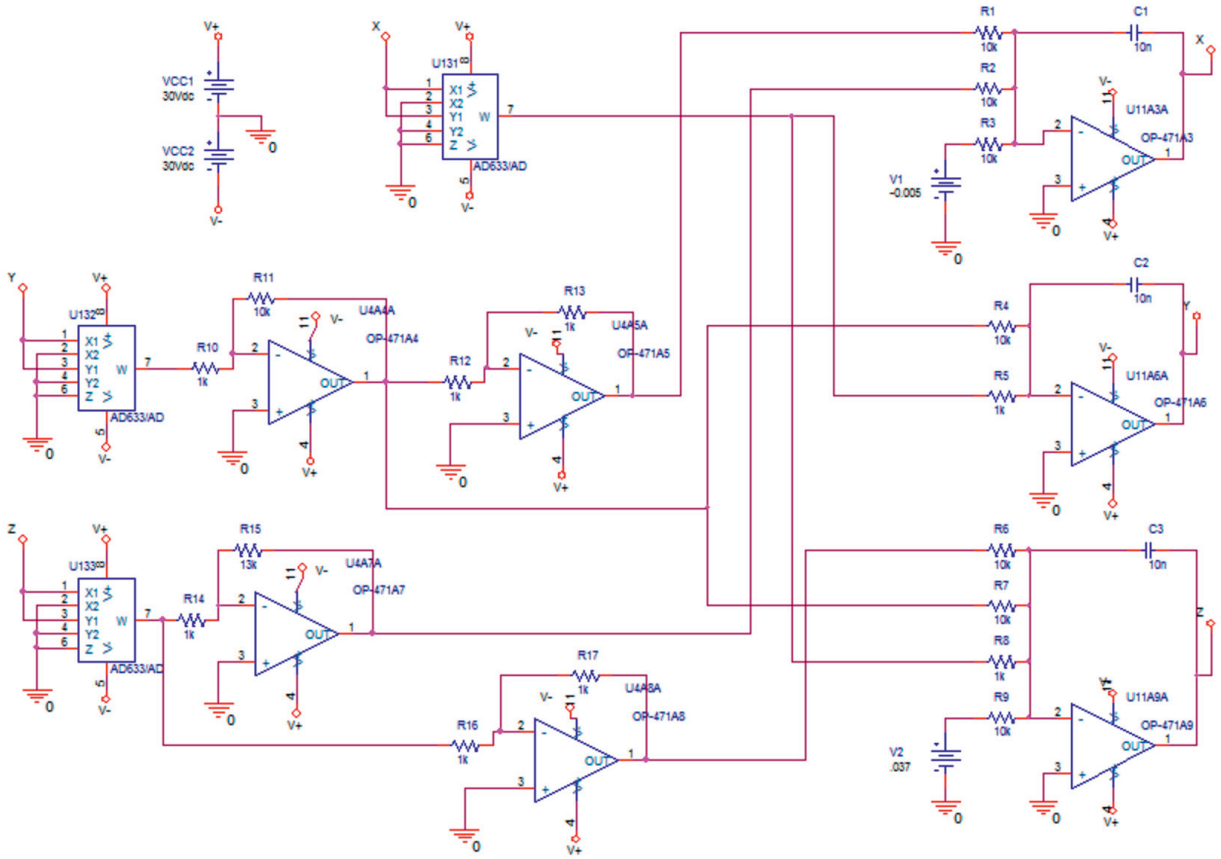

Figure 5: Schematic of the pure nonlinear system's designed circuit. In the designed circuits, all used elements are analogs. Op-Amps are used as integrators. Besides, they are also used for regulating the coefficients of nonlinear terms. Capacitors and resistors are the other analog elements in the circuit. The circuit is simulated in PSpice software.

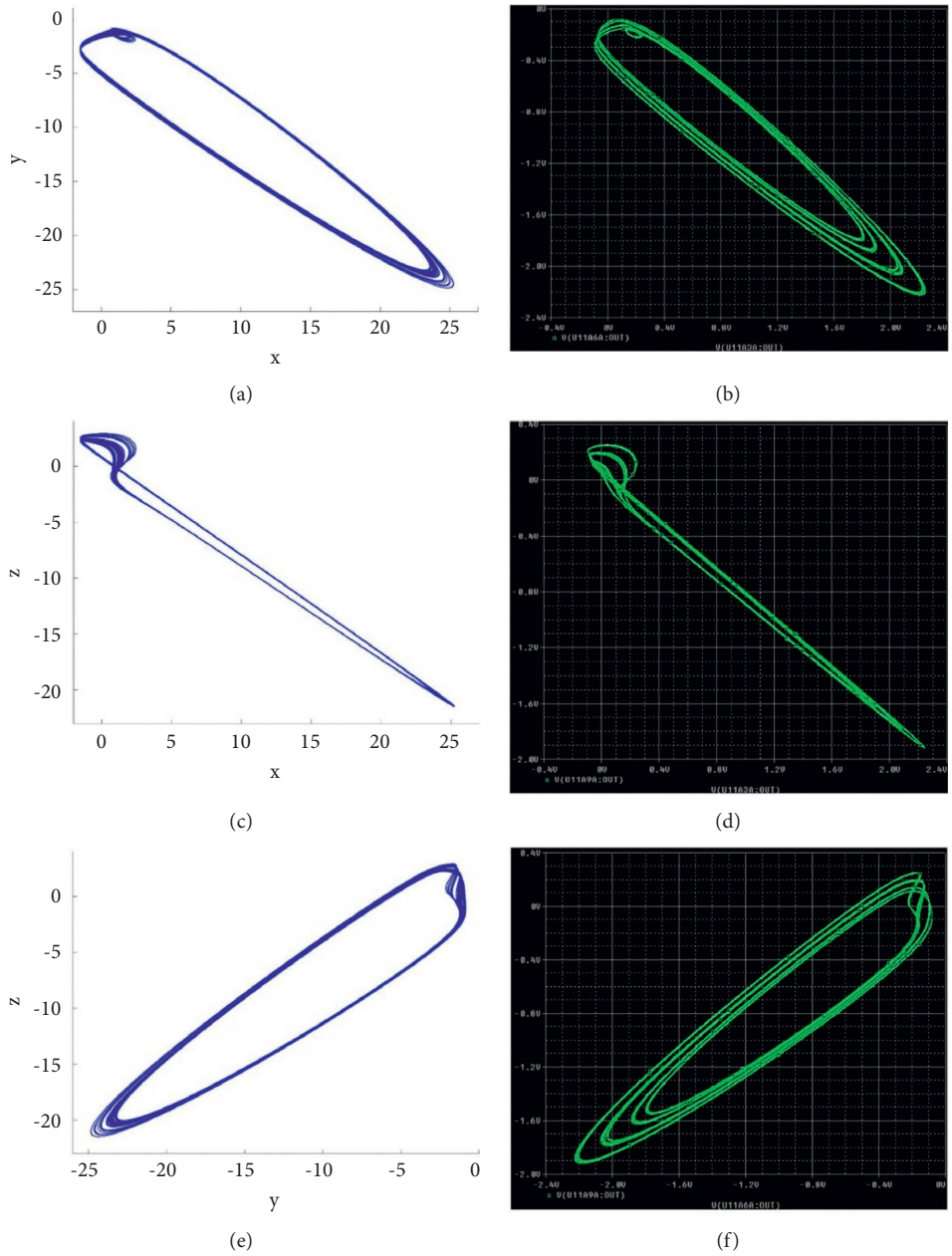

FIGURE 6: The results of Matlab and PSpice simulations for the system's attractor when $a = 0.5$ and $b = -3.7$. (a), (c), and (e) are related to the Matlab simulations when (b), (d), and (f) are generated by the analog circuit designed in PSpice. (a, b) The attractor's projection in the XY plane, (c, d) the attractor's shadow in the XZ plane, and (e, f) the attractor's projection in the surface of the YZ.

(SaEn). Accepting this definition, SaEn is applied to estimate the complexity of the system's time series, as reviewed in the Introduction section. SaEn tries to measure the predictability of $(t+1)th$ samples of time series when the previous samples $(1, 2, \ldots, t)$ are observed. The algorithm of calculating SaEn can be read in [37]. To calculate the algorithm of SaEn, $m = 2$ and $r = 0.2$ are considered. The algorithm is applied to the oscillator's attractors (the x variable time series) for ranges of the parameters (a and b). The initial conditions are considered $(0, 0, 0)$ and the transient time parts of the time series are emitted before calculating SaEn. The results of SaEn values can be observed in Figure 7. The attractor is a fixed point in parameters that SaEn values are zero. A trend can be seen that increasing a, at first, causes an increase in SaEn and then decreases it. In comparison with Figure 2, generally chaotic states of the system have more sample entropy values than periodic ones. Besides, a trend also can be observed that decreasing b parameter values increases SaEn values. Comparing this trend with the bifurcation diagram reveals that the chaotic regions generally have more complexity.

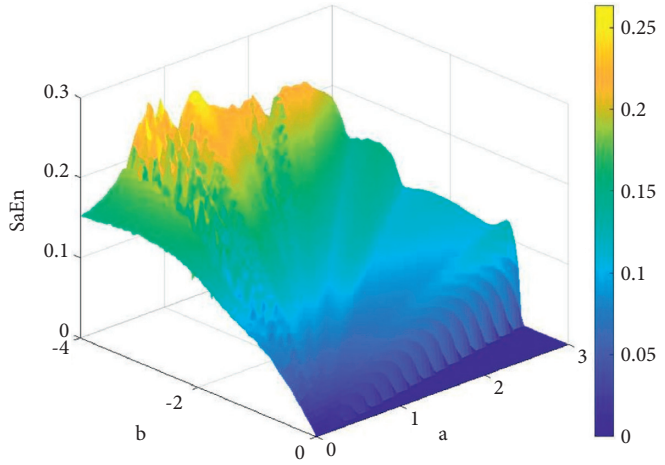

FIGURE 7: The sample entropy is used for assessing the oscillator's signals complexities for a range of the system's parameters. A trend can be seen that decreasing b and increasing a values result in increasing the sample entropy.

5. Impulsive Control

Here, the pure nonlinear oscillator is controlled using impulsive control. In the first step, the system under impulsive control can be described as follows [65–67]:

$$\begin{aligned} \dot{X} &= f(t, X) \\ &= AX + \Phi(X), \\ \Delta X &= X(t^{+}) - X(t^{-}) \\ &= U(k, X), \\ t &= T_k, \\ k &= 1, 2, \ldots \end{aligned} \tag{6}$$

When $f: R_{+} \times R^n \longrightarrow R^n$ is continuous, $U: R^n \times R^n \longrightarrow R^n$ is continuous; $X \in R^n$ is the vector of state variables; and $0 < T_1 < T_2 < \ldots < T_K < T_{K+1} < \ldots, T_{K \longrightarrow \infty}$ *as* $k \longrightarrow \infty$. AX, in general, represents linear terms of systems when $\Phi(X)$ contains nonlinear terms.

Definition 1. Assuming $V: R_{+} \times R^n \longrightarrow R_{+}$, then V is said to belong to the class V_0, if

(1) V is continuous in $(T_{k-1}, T_k] \times R^n$ and for each $X \in R^n$, $k = 1, 2, \ldots$, $(t, Y) \longrightarrow (T_k^{+}, X)$ $lim\, V(t, Y) = V(T_k^{+}, X)$ exists

(2) V is locally Lipschitzian in X

Definition 2. For $(t, X) \in (T_{i-1}, T_i]] \times R^n$, it is considered:

$$\begin{aligned} D^{+}V(t, X) \triangleq h \longrightarrow 0 + \limsup \frac{1}{h} [V(t + h, X \\ + hf(t, X)) - V(t, X)]. \end{aligned} \tag{7}$$

Definition 3 (comparison system). Let $V \in V0$ and assume that

$$D^{+}V(t, X) \leq g(t, V(t, X)),\ t \neq T_k;\ \text{and}\ V(t, X + U(k, X)) \leq \Psi k(V(t, X)),\ t = T_k, \tag{8}$$

where $g: R_{+} \times R_{+} \longrightarrow R$ is continuous and $\Psi k: R_{+} \longrightarrow R_{+}$ is nondecreasing. Then the following system is the comparison system of Eq. (6):

$$\begin{aligned} \omega &= g(t, \omega),\ t \neq T_k \omega(T_k^{+}) \\ &= \Psi k(\omega(T_k))\omega(T_0^{+}) \\ &= \omega 0 \geq 0. \end{aligned} \tag{9}$$

Theorem 1. *These three conditions are assumed:*

(1) $V: R^n \times R^n \longrightarrow R_{+}$, $V \in V0$, $K(t)D^{+}V(t, X) + D^{+}K(t)V(t, X) \leq g(t, K(t)V(t, X))$, $t \triangleq \tau k$, *when* g *is continuous in* $(T_{k-1}, T_k] \times R^n$ *for each* $x \in R^n$, $k = 1, 2, \ldots$, $(t, y) \longrightarrow (T_k^{+}, x) \lim g(t, y) = g(T_k^{+}, x)$ *exists.* $K(t) \geq m > 0$, $t \longrightarrow T_k^{-} \lim K(t) = K(T_k)$, $t \longrightarrow T_k^{+} \lim K(t)$ *exists,* $k = 1, 2, \ldots, D^{+}K(t) = h \longrightarrow 0^{+} \limsup (1/h)[K(t + h) - K(t)]$

(2) $K(T_k + 0)V(T_k + 0, X + U(k, X)) \leq \Psi k(K(T_k)\, V(T_k, X))$, $k = 1, 2, \ldots$

(3) $V(t, 0) = 0$ *and* $\alpha(|X|) \leq V(t, X)$ *on* $R_{+} \times R^n$, *when* $\alpha(\cdot) \in \aleph$ *(continuous strictly increasing function class* $\alpha: R_{+} \longrightarrow R_{+}$ *so that* $\alpha(0) = 0$*) are satisfied. Next, the global asymptotic stability for the trivial solution* $\omega = 0$ *of the comparison system implies global asymptotic stability of impulsive system (6) trivial solution*

Theorem 2. *Let $g(t, \omega) = \dot{\lambda}(t)\omega, \Psi k(\omega) = d_k\omega, d_k \geq 0$ for all $k \geq 1$. consequently, system (6) origin is global asymptotically stable if Theorem 1 conditions and the following conditions are held:*

(1) $\lambda(t)$ is nondecreasing, $t \longrightarrow T_k^+ \lim \lambda(t) = \lambda(T_k)$, $t \longrightarrow T_k^+ \lim \lambda(t) = \lambda(T_k^+)$ exists, for all $k = 1, 2, \ldots$

(2) $sup_i\ [d_I exp(\lambda(T_{i+1}) - \lambda(T_i^+))] = \varepsilon_0 < \infty$

(3) There exists a $r > 1$ such that $\lambda(T_{2k+3}) + \lambda(T_{2k+2}) + ln(rd_{2k+2} + d_{2k+1}) \leq \lambda(T_{2k+2}^+) + \lambda(T_{2k+2}^+)$ is held for all $d_{2k+2}d_{2k+1} \neq 0$, $k = 1, 2, \ldots$, or there exists an $r > 1$ so that $\lambda(T_{k+1}) + ln(rd_k) \leq \lambda(T_k^+)$ for all k

(4) $V(t, 0) = 0$ and there exists $\alpha(\cdot)$ in class N such that $\alpha(\|X\|) \leq V(t, X)$

Theorem 3. *The origin of the introduced pure nonlinear chaotic system is asymptotically stable if there exists a $\xi > 1$ and a differentiable at $t \neq T_k$, and nonincreasing function $K(t)$ which satisfies the following:*

$$-\frac{\dot{K(t)}}{K(t)} \leq q + r \leq \frac{1}{(1+\varepsilon)\Delta 2}\ln\left(\left(\frac{K(T_{2i}^+)K(T_{2i-1}^+)}{K(T_{2i+1})K(T_{2i})\xi d^2}\right)\right) \text{ or}$$

$$-\frac{\dot{K(t)}}{K(t)} \leq q + r \leq \frac{1}{\max(\Delta 1, \Delta 2)}\ln\left(\frac{K(T_i^+)}{K(T_{i+1})\xi\ d}\right),$$

$$r = \begin{cases} 0, if \quad P = I, \\ 2M\sqrt{\dfrac{\lambda_2}{\lambda_1}}\ if \quad P \neq I, \end{cases} \tag{10}$$

q is the $(A + P^{-1}A^TP)$ largest eigenvalue assuming P is a positive definite symmetric matrix and $\lambda_1 > 0$ and $\lambda_2 > 0$ are the smallest and the largest eigenvalues of P, respectively. $\rho(A)$ denote the spectral radius of A: $d = \rho^2(I + B)$. M for the pure nonlinear chaotic system considered so that $|x_{(t)}| < M, |y_{(t)}| < M, |z_{(t)}| < M.K(t)$. It is as in Theorem 1, T_i: $i = 1, 2, \ldots$ are varying but satisfy the following:

$$\begin{aligned} \Delta 1 &= \sup_{1 \leq j < \infty}\left(T_{2j+1} - T_{2j}\right) < \infty, \\ \Delta 2 &= \sup_{1 \leq j < \infty}\left(T_{2j} - T_{2j-1}\right) < \infty. \end{aligned} \tag{11}$$

Furthermore, for a given constant ε,

$$T_{2j+1} - T_{2j} \leq \varepsilon\left(T_{2j} - T_{2j-1}\right)\ \forall j \in 1, 2, \ldots, \infty. \tag{12}$$

This theorem's proof can be seen in [66].

Remark 1. Theorem 3 also gives an estimate for the upper bound. $\Delta 1_{max}$ and $\Delta 2_{max}$ of impulsive intervals are given by

$$\Delta 1 = \frac{1}{(1+\varepsilon)(q + 2|a\alpha|)}\ln\left(\frac{K(T_{2i}^+)K(T_{2i-1}^+)}{K(T_{2i+1})K(T_{2i})\xi d^2}\right), \tag{13}$$

$$\Delta 2 = \varepsilon\Delta 1.$$

The introduced pure nonlinear system when $a = 0.5$ and $b = 2.3$ are set is considered. According to the second section, this system has eight equilibrium points. Assuming (x^*, y^*, z^*) as an equilibrium point of the system, the system equations considering $x_1 = x - x^*$, $y_1 = y - y^*$, $z_1 = z - z^*$ can be rewritten as follows:

$$\begin{aligned} \dot{x_1} &= 1.3z_1^2 + 2.6z^*z_1 + 1.3z^{*2} - y_1^2 - 2y^*y_1 - y^{*2} + a, \\ \dot{y_1} &= y_1^2 + 2y^*y_1 + y^{*2} - x_1^2 - 2x^*x_1 - x^{*2}, \\ \dot{z_1} &= y_1^2 + 2y^*y_1 + y^{*2} - x_1^2 - 2x^*x_1 - x^{*2} + 0.1z_1^2 + 0.2z^*z_1 + 0.1z^{*2} + b. \end{aligned} \tag{14}$$

Equilibrium $(x^* = +\sqrt{30.4}, y^* = -\sqrt{30.4}, z^* = -\sqrt{23})$ is considered to be stabilized. Without losing generosity for stabilizing equilibrium points of the system, the same method can be applied to the other equilibria of the pure nonlinear system. In this way, considering (6) and (12), for the equilibrium point $(x^* = +\sqrt{30.4}, y^* = -\sqrt{30.4}, z^* = -\sqrt{23})$, equations can be rewritten as follows:

$$\dot{X} = AX + \Phi(X),$$

$$A = \begin{pmatrix} 0 & -2y^* & 2.6z^* \\ -2x^* & 2y^* & 0 \\ -2x^* & 2y^* & 0.2z^* \end{pmatrix}$$

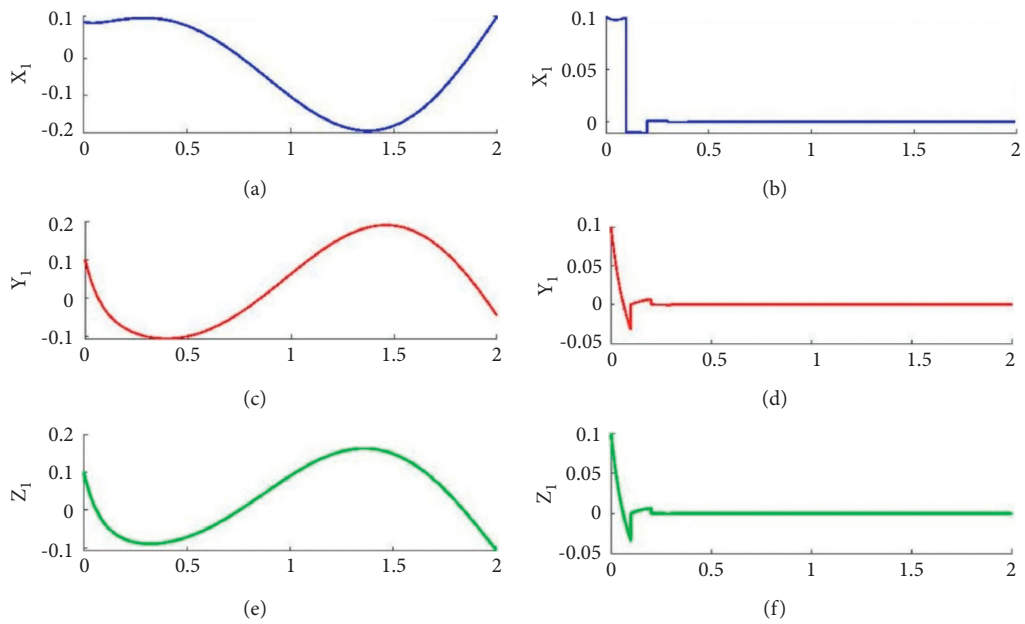

Figure 8: For the initial condition $(0.1, 0.1, 0.1)$, time series of x_1, y_1, and z_1 of the system demonstrated in Equation (12) are plotted in (a), (b), and (c), respectively. The transient signals of, x_1, y_1, and z_1 for this system under the impulsive controller (Equation (13)) are plotted in (d), (e), and (f), respectively.

$$
\begin{aligned}
&= \begin{pmatrix} 0 & 2\sqrt{30.4} & -2.6\sqrt{23} \\ -2\sqrt{30.4} & -2\sqrt{30.4} & 0 \\ -2\sqrt{30.4} & -2\sqrt{30.4} & -0.2\sqrt{23} \end{pmatrix}, \\
\Phi(X) &= \begin{bmatrix} 1.3z_1^2 - y_1^2 \\ y_1^2 - x_1^2 \\ y_1^2 - x_1^2 + 0.1z_1^2 \end{bmatrix}, \\
U(k, X) &= BX, \\
t &= T_k, k = 1, 2, \ldots
\end{aligned} \tag{15}
$$

Considering $K(t) = 1$, $\varepsilon = 1$, $\xi = 1.1$, $B = \begin{pmatrix} s = -1.1 & 0 & 0 \\ 0 & -1 & 0 \\ 0 & 0 & -1 \end{pmatrix}$ and $P = I$, then $d = (s+1)^2 = 0.01$, $q = 23.86$ $(T_{2j+1} - T_{2j}) = (T_{2j} - T_{2j-1}) = \Delta < (\Delta 1 = \Delta 2 = -\ln(\xi\ d)/q = 0.1890 \longrightarrow (\Delta$ is considered $0.1))$. The stabilized system numerical simulations are plotted in Figure 8. Figures 8(a)–8(c) demonstrate the time series of x_1, y_1, and z_1, respectively, for the oscillator described in Eq. 12. The time series of x_1, y_1, and z_1 for the stabilized system using the impulsive controller (based on Eq. 13) are demonstrated in Figures 8(d)–8(f), respectively.

6. Conclusion

Here, a pure nonlinear 3D system was presented. It was observed that the system could generate periodic, torus, and chaotic time series. Analytical analysis revealed that the oscillator has eight unstable equilibrium points for a set of parameters. The basin of attraction diagrams showed for this set of parameters that the system attractor is self-excited. The pure nonlinear system's feasibility was investigated with an analog circuit built by simple elements like capacitors and Op-Amps. Changing parameters' values revealed that the system could generate time series with a wide range of complexities. A possible solution to system stabilization was described by using the impulsive controller on the system. For this system, when both constants (parameters a and b) were equal to zero, the system had an unbounded solution. According to the authors' best knowledge, no pure nonlinear quadratic system has been introduced before with no constant values in its equations. Therefore, searching for such a system can be interesting for future research.

Data Availability

All the numerical simulation parameters are mentioned in the respective text part, and there are no additional data requirements for the simulation results.

Conflicts of Interest

The authors declare that there are no conflicts of interest.

Acknowledgments

This work was funded by the Center for Nonlinear Systems, Chennai Institute of Technology, India, vide funding number CIT/CNS/2021/RP-015.

References

[1] H. Bao, M. Chen, H. Wu, and B. Bao, "Memristor Initial-Boosted Coexisting Plane Bifurcations and its Extreme Multi-Stability Reconstitution in Two-Memristor-Based Dynamical System," *Science China Technological Sciences*, vol. 63, pp. 1–11, 2019.

[2] Z. Faghani, F. Nazarimehr, S. Jafari, and J. C. Sprott, "Simple chaotic systems with specific analytical solutions," *International Journal of Bifurcation and Chaos*, vol. 29, no. 9, Article ID 1950116, 2019.

[3] F. Nazarimehr and J. C. Sprott, "Investigating chaotic attractor of the simplest chaotic system with a line of equilibria," *The European Physical Journal - Special Topics*, vol. 229, no. 6-7, pp. 1289–1297, 2020.

[4] M. Chen, J. Qi, H. Wu, Q. Xu, and B. Bao, "Bifurcation analyses and hardware experiments for bursting dynamics in non-autonomous memristive fitzhugh-nagumo Circuit," *Science China Technological Sciences*, vol. 63, pp. 1–10, 2020.

[5] A. Bahramian, F. Parastesh, V.-T. Pham, T. Kapitaniak, S. Jafari, and M. Perc, "Collective behavior in a two-layer neuronal network with time-varying chemical connections that are controlled by a Petri net," *Chaos: An Interdisciplinary Journal of Nonlinear Science*, vol. 31, no. 3, Article ID 033138, 2021.

[6] A. Bahramian, A. Nouri, F. Towhidkhah, H. Azarnoush, and S. Jafari, "Introducing a nonlinear coupling for central pattern generator: improvement on robustness by expanding basin of attraction and performance by decreasing the transient time," *Journal of Vibration and Control*, vol. 26, no. 7-8, pp. 377–386, 2020.

[7] V.-T. Pham, S. Jafari, C. Volos, X. Wang, and S. M. R. H. Golpayegani, "Is that really hidden? The presence of complex fixed-points in chaotic flows with no equilibria," *International Journal of Bifurcation and Chaos*, vol. 24, no. 11, Article ID 1450146, 2014.

[8] Z. Wei, I. Moroz, J. C. Sprott, A. Akgul, and W. Zhang, "Hidden hyperchaos and electronic circuit application in a 5D self-exciting homopolar disc dynamo," *Chaos: An Interdisciplinary Journal of Nonlinear Science*, vol. 27, no. 3, Article ID 033101, 2017.

[9] J. C. Sprott and B. Munmuangsaen, "Comment on "A hidden chaotic attractor in the classical Lorenz system"," *Chaos, Solitons & Fractals*, vol. 113, pp. 261-262, 2018.

[10] M. Molaie, S. Jafari, J. C. Sprott, and S. M. R. H. Golpayegani, "Simple chaotic flows with one stable equilibrium," *International Journal of Bifurcation and Chaos*, vol. 23, no. 11, Article ID 1350188, 2013.

[11] C. Feng, Q. Huang, and Y. Liu, "Jacobi analysis for an unusual 3D autonomous system," *International Journal of Geometric Methods in Modern Physics*, vol. 17, no. 04, Article ID 2050062, 2020.

[12] A. Giakoumis, C. Volos, A. J. M. Khalaf et al., "Analysis, synchronization and microcontroller implementation of a new quasiperiodically forced chaotic oscillator with megastability," *Iranian Journal of Science and Technology, Transactions of Electrical Engineering*, vol. 44, no. 1, pp. 31–45, 2020.

[13] K. Sun and J. C. Sprott, "Periodically forced chaotic system with signum nonlinearity," *International Journal of Bifurcation and Chaos*, vol. 20, no. 05, pp. 1499–1507, 2010.

[14] B. Bao, J. Luo, H. Bao, C. Chen, H. Wu, and Q. Xu, "A simple nonautonomous hidden chaotic system with a switchable stable node-focus," *International Journal of Bifurcation and Chaos*, vol. 29, no. 12, Article ID 1950168, 2019.

[15] T. Banerjee, D. Biswas, and B. C. Sarkar, "Design and analysis of a first order time-delayed chaotic system," *Nonlinear Dynamics*, vol. 70, no. 1, pp. 721–734, 2012.

[16] H. G. Wu, Y. Ye, B. C. Bao, M. Chen, and Q. Xu, "Memristor initial boosting behaviors in a two-memristor-based hyperchaotic system," *Chaos, Solitons & Fractals*, vol. 121, pp. 178–185, 2019.

[17] C. Li, G. Chen, J. Kurths, T. Lei, and Z. Liu, "Dynamic transport: from bifurcation to multistability," *Communications in Nonlinear Science and Numerical Simulation*, vol. 95, Article ID 105600, 2021.

[18] W. J. Sanders, "The topology of chaos: alice in stretch and squeezeland," *Mathematics Teacher*, vol. 96, p. 218, 2003.

[19] M. Hua, S. Yang, Q. Xu, M. Chen, H. Wu, and B. Bao, "Symmetrically Scaled Coexisting Behaviors in Two Types of Simple Jerk Circuits," *Circuit World*, vol. 47, 2020.

[20] S. Zhang, J. Zheng, X. Wang, and Z. Zeng, "Multi-scroll hidden attractor in memristive HR neuron model under electromagnetic radiation and its applications," *Chaos: An Interdisciplinary Journal of Nonlinear Science*, vol. 31, no. 1, Article ID 011101, 2021.

[21] E. C. Díaz-González, J.-A. López-Rentería, E. Campos-Cantón, and B. Aguirre-Hernández, "Maximal unstable dissipative interval to preserve multi-scroll attractors via multi-saturated functions," *Journal of Nonlinear Science*, vol. 26, pp. 1833–1850, 2016.

[22] J. P. Singh, J. Koley, K. Lochan, and B. K. Roy, "Presence of megastability and infinitely many equilibria in a periodically and quasi-periodically excited single-link manipulator," *International Journal of Bifurcation and Chaos*, vol. 31, no. 2, Article ID 2130005, 2021.

[23] A. Sambas, S. Vaidyanathan, E. Tlelo-Cuautle et al., "A 3-D multi-stable system with a peanut-shaped equilibrium curve: circuit design, FPGA realization, and an application to image encryption," *IEEE Access*, vol. 8, pp. 137116–137132, 2020.

[24] V. P. Thoai, M. S. Kahkeshi, V. V. Huynh, A. Ouannas, and V.-T. Pham, "A nonlinear five-term system: symmetry, chaos, and prediction," *Symmetry*, vol. 12, no. 5, p. 865, 2020.

[25] M. D. Vijayakumar, A. Bahramian, H. Natiq, K. Rajagopal, and I. Hussain, "A chaotic quadratic bistable hyperjerk system with hidden attractors and a wide range of sample entropy: impulsive stabilization," *International Journal of Bifurcation and Chaos*, vol. 31, Article ID 2150253, 2021.

[26] J. Kengne, S. Jafari, Z. T. Njitacke, M. Yousefi Azar Khanian, and A. Cheukem, "Dynamic analysis and electronic circuit implementation of a novel 3D autonomous system without linear terms," *Communications in Nonlinear Science and Numerical Simulation*, vol. 52, pp. 62–76, 2017.

[27] V. T. Pham, S. Jafari, C. Volos, and L. Fortuna, "Simulation and experimental implementation of a line-equilibrium system without linear term," *Chaos, Solitons & Fractals*, vol. 120, pp. 213–221, 2019.

[28] Y. Xu and Y. Wang, "A new chaotic system without linear term and its impulsive synchronization," *Optik*, vol. 125, no. 11, pp. 2526–2530, 2014.

[29] Z. T. Njitacke, R. L. T. Mogue, G. D. Leutcho, T. Fonzin Fozin, and J. Kengne, "Heterogeneous multistability in a novel system with purely nonlinear terms," *International Journal of Electronics*, pp. 1–17, 2020.

[30] V. Carbajal-Gómez, E. Tlelo-Cuautle, R. Trejo-Guerra, C. Sánchez-López, and J. Munoz-Pacheco, "Experimental synchronization of multiscroll chaotic attractors using current-feedback operational amplifiers," *Nonlinear Science Letters B: Chaos, Fractal, Synchronization*, vol. 1, pp. 37–42, 2011.

[31] F. Hellmann, P. Schultz, P. Jaros et al., "Network-induced multistability through lossy coupling and exotic solitary states," *Nature Communications*, vol. 11, pp. 592–599, 2020.

[32] E. Tlelo-Cuautle, A. Dalia Pano-Azucena, O. Guillén-Fernández, and A. Silva-Juárez, "Synchronization and applications of fractional-order chaotic systems," *Analog/Digital Implementation of Fractional Order Chaotic Circuits and Applications*, pp. 175–201, Springer, Cham, Switzerland, 2020.

[33] E. Tlelo-Cuautle, O. Guillén-Fernández, J. de Jesus Rangel-Magdaleno, A. Melendez-Cano, J. C. Nuñez-Perez, and L. G. de la Fraga, "FPGA implementation of chaotic oscillators, their synchronization, and application to secure communications," *Recent Advances in Chaotic Systems and Synchronization*, pp. 301–328, Academic Press, Cambridge, MA, USA, 2019.

[34] E. Tlelo-Cuautle, J. D. Díaz-Muñoz, A. M. González-Zapata et al., "Chaotic image encryption using hopfield and hindmarsh-rose neurons implemented on FPGA," *Sensors*, vol. 20, no. 5, p. 1326, 2020.

[35] H. Natiq, S. Banerjee, and M. R. M. Said, "Cosine chaotification technique to enhance chaos and complexity of discrete systems," *The European Physical Journal - Special Topics*, vol. 228, no. 1, pp. 185–194, 2019.

[36] L. Liu, C. Du, L. Liang, and X. Zhang, "A high Spectral Entropy (SE) memristive hidden chaotic system with multitype quasi-periodic and its circuit," *Entropy*, vol. 21, no. 10, p. 1026, 2019.

[37] J. S. Richman and J. R. Moorman, "Physiological time-series analysis using approximate entropy and sample entropy," *American Journal of Physiology. Heart and Circulatory Physiology*, vol. 278, pp. H2039–H2049, 2000.

[38] J. N. Weiss, A. Garfinkel, M. L. Spano, and W. L. Ditto, "Chaos and chaos control in biology," *Journal of Clinical Investigation*, vol. 93, no. 4, pp. 1355–1360, 1994.

[39] T. Kapitaniak, L. Kocarev, and L. O. Chua, "Controlling chaos without feedback and control signals," *International Journal of Bifurcation and Chaos*, vol. 3, no. 2, pp. 459–468, 1993.

[40] E. Ott, C. Grebogi, and J. A. Yorke, "Controlling chaos," *Physical Review Letters*, vol. 64, no. 11, pp. 1196–1199, 1990.

[41] X. Li, T. Caraballo, R. Rakkiyappan, and X. Han, "On the stability of impulsive functional differential equations with infinite delays," *Mathematical Methods in the Applied Sciences*, vol. 38, no. 14, pp. 3130–3140, 2015.

[42] X. Yang, X. Li, X. Li, Q. Xi, and P. Duan, "Review of stability and stabilization for impulsive delayed systems," *Mathematical Biosciences and Engineering*, vol. 15, no. 6, pp. 1495–1515, 2018.

[43] X. Li, J. Shen, and R. Rakkiyappan, "Persistent impulsive effects on stability of functional differential equations with finite or infinite delay," *Applied Mathematics and Computation*, vol. 329, pp. 14–22, 2018.

[44] Z. Yang, W. Zhou, and T. Huang, "Input-to-state stability of delayed reaction-diffusion neural networks with impulsive effects," *Neurocomputing*, vol. 333, pp. 261–272, 2019.

[45] X. Li, D. O'Regan, and H. Akca, "Global exponential stabilization of impulsive neural networks with unbounded continuously distributed delays," *IMA Journal of Applied Mathematics*, vol. 80, no. 1, pp. 85–99, 2015.

[46] J. Hu, G. Sui, X. Lv, and X. Li, "Fixed-time control of delayed neural networks with impulsive perturbations," *Nonlinear Analysis Modelling and Control*, vol. 23, no. 6, pp. 904–920, 2018.

[47] D. Peng, X. Li, R. Rakkiyappan, and Y. Ding, "Stabilization of stochastic delayed systems: event-triggered impulsive control," *Applied Mathematics and Computation*, vol. 401, Article ID 126054, 2021.

[48] X. Li, J. Shen, H. Akca, and R. Rakkiyappan, "LMI-based stability for singularly perturbed nonlinear impulsive differential systems with delays of small parameter," *Applied Mathematics and Computation*, vol. 250, pp. 798–804, 2015.

[49] M. Li, H. Chen, and X. Li, "Exponential stability of nonlinear systems involving partial unmeasurable states via impulsive control," *Chaos, Solitons & Fractals*, vol. 142, Article ID 110505, 2021.

[50] X. Tan, J. Cao, and X. Li, "Event-based impulsive control for nonlinear systems and its application to synchronization of Chua's circuit," *IMA Journal of Mathematical Control and Information*, vol. 37, pp. 82–104, 2018.

[51] X. Li, H. Zhu, and S. Song, "Input-to-state stability of nonlinear systems using observer-based event-triggered impulsive control," *IEEE Transactions on Systems Man Cybernetics Systems*, vol. 51, 2020.

[52] D. Yang, X. Li, and J. Qiu, "Output tracking control of delayed switched systems via state-dependent switching and dynamic output feedback," *Nonlinear Analysis: Hybrid Systems*, vol. 32, pp. 294–305, 2019.

[53] D. Yang, X. Li, J. Shen, and Z. Zhou, "State-dependent switching control of delayed switched systems with stable and unstable modes," *Mathematical Methods in the Applied Sciences*, vol. 41, no. 16, pp. 6968–6983, 2018.

[54] S. Peng, J. Zhang, J. Zhu, J. Lu, and X. Li, "Exact exponential synchronization rate of high-dimensional Kuramoto models with identical oscillators and digraphs," 2021, https://arxiv.org/abs/2102.03817.

[55] P. Wang, X. Li, N. Wang, Y. Li, K. Shi, and J. Lu, "Almost periodic synchronization of quaternion-valued fuzzy cellular neural networks with leakage delays," *Fuzzy Sets and Systems*, vol. 426, 2021.

[56] Y. Zhao, X. Li, and J. Cao, "Global exponential stability for impulsive systems with infinite distributed delay based on flexible impulse frequency," *Applied Mathematics and Computation*, vol. 386, Article ID 125467, 2020.

[57] F. Nazarimehr, S. Jafari, G. Chen et al., "A tribute to J. C. Sprott," *International Journal of Bifurcation and Chaos*, vol. 27, no. 14, Article ID 1750221, 2017.

[58] Z. Wei, "Dynamical behaviors of a chaotic system with no equilibria," *Physics Letters A*, vol. 376, no. 2, pp. 102–108, 2011.

[59] X. Wang and G. Chen, "A chaotic system with only one stable equilibrium," *Communications in Nonlinear Science and Numerical Simulation*, vol. 17, no. 3, pp. 1264–1272, 2012.

[60] A. Sambas, S. Vaidyanathan, T. Bonny et al., "Mathematical model and FPGA realization of a multi-stable chaotic dynamical system with a closed butterfly-like curve of equilibrium points," *Applied Sciences*, vol. 11, no. 2, p. 788, 2021.

[61] Z. Wang, Z. Wei, K. Sun et al., "Chaotic flows with special equilibria," *The European Physical Journal - Special Topics*, vol. 229, no. 6-7, pp. 905–919, 2020.

[62] Q. Wan, Z. Zhou, W. Ji, C. Wang, and F. Yu, "Dynamic analysis and circuit realization of a novel no-equilibrium 5D memristive hyperchaotic system with hidden extreme multistability," *Complexity*, vol. 2020, Article ID 7106861, 2020.

[63] S. Nag Chowdhury and D. Ghosh, "Hidden attractors: a new chaotic system without equilibria," *The European Physical Journal - Special Topics*, vol. 229, no. 6-7, pp. 1299–1308, 2020.

[64] X. Zhang and C. Wang, "Multiscroll hyperchaotic system with hidden attractors and its circuit implementation," *International Journal of Bifurcation and Chaos*, vol. 29, no. 9, Article ID 1950117, 2019.

[65] X. He, C. Li, X. Pan, and M. Peng, "Impulsive control and Hopf bifurcation of a three-dimensional chaotic system," *Journal of Vibration and Control*, vol. 20, no. 9, pp. 1361–1368, 2014.

[66] J. Sun and Y. Zhang, "Impulsive control of Lorenz systems," in *Proceedings of the Fifth World Congress on Intelligent Control and Automation*, pp. 71–73, IEEE, Hangzhou, China, June 2004.

[67] X. Li, X. Yang, and T. Huang, "Persistence of delayed cooperative models: impulsive control method," *Applied Mathematics and Computation*, vol. 342, pp. 130–146, 2019.